



## DFT calculations for corrosion inhibition of copper by tetrazole derivatives

M. Rajendran\* and D. Devapiriam

Department of Chemistry, Centre for Research and Post Graduate Studies in Chemistry, N. M. S. S. Vellaichamy Nadar College (Autonomous), Nagamalai, Madurai, Tamilnadu, India

### ABSTRACT

Corrosion inhibition of Copper through two Tetrazole derivatives has been elucidated by means of Density Functional Theory (DFT) at the B3LYP/6-311G(d,p) basis set level. The calculated structural parameters were correlated to the inhibition efficiency of the frontier molecular orbital energies  $E_{HOMO}$  (Energy of highest occupied molecular orbital),  $E_{LUMO}$  (Energy of lowest unoccupied molecular orbital), energy gap ( $\Delta E$ ), dipole moment ( $\mu$ ), hardness ( $\eta$ ), softness ( $\sigma$ ), the absolute electronegativity ( $\chi$ ), the electrophilicity index ( $\omega$ ) and the fraction of electrons transferred ( $\Delta N$ ) from the tetrazole molecule to Copper. The local reactivity has been analysed through the Fukui and condensed softness indices in order to predict both the reactive centres and to know the possible sites of nucleophilic and electrophilic attack. The theoretical results, predicted using DFT-based reactivity indexes, are in good agreement with the published experimental results.

**Keywords:** DFT, G09, corrosion inhibition, Tetrazole, Fukui function

### INTRODUCTION

Copper is one of the most important material used widely in different industries, because of its excellent conductivity, good mechanical workability and relatively low cost and reactivity. However, it easily undergoes corrosion in various environmental conditions. It has been reported that many heterocyclic compounds containing heteroatom like N, O, and S have been proved to be effective inhibitors for the corrosion. The corrosion inhibition property of these compounds is attributed to their molecular structure. The use of inhibitors is one of the most practical methods for protecting metals or alloys from corrosion. Inhibitors are chemicals that often work by adsorbing themselves on the metallic surface by forming a film [1-3]. The inhibitor properties of two tetrazole derivatives namely, 1-phenyl-1,2,3,4-tetrazole-5-thiol (Tetrazole-1) and 5-Benzylthio-1-phenyl-1,2,3,4-tetrazole (Tetrazole-2) have been reported [4]. The inhibition efficiency of such inhibitors depends essentially on the structure of the inhibitor itself, which include the number of active adsorption centres in the molecule, the nature of the metal and the aggressive solution. The structure and the lone pairs of electron in the heteroatoms are important features that determine the adsorption of these molecules on the metallic surface. The effect of inhibitors adsorbed on metallic surfaces in acid solutions, is to slow down the cathodic reaction as well as anodic process of dissolution of metals. Such effect is obtained by forming a barrier of diffusion or by means of blockage of the reaction sites and thereby reducing the corrosion rate [5]. Many substituted tetrazoles have recently been studied in much detail as effective corrosion inhibitors for metal in acid media [6-8]. Nitrogen and sulphur containing heterocyclic compounds and its derivative compounds may act as inhibitors for copper dissolution due to the chelating action of heterocyclic molecules and the formation of a physical blocking barrier on the copper surface [9-11].

Recently, quantum chemical calculations have been found to be one of the most powerful tools for studying the mechanism of inhibition of the corrosion of metal by organic inhibitors [12-15]. A perusal of literature reveals that corrosion inhibition efficiency of tetrazole derivative has not been reported using quantum chemical calculations. The present work investigate the inhibition efficiency of these compounds based on theoretical studies using chemical reactivity descriptors such as  $E_{HOMO}$  (Energy of highest occupied molecular orbital),  $E_{LUMO}$  (Energy of

lowest unoccupied molecular orbital), energy gap ( $\Delta E$ ), dipole moment ( $\mu$ ), hardness ( $\eta$ ), softness ( $\sigma$ ), the absolute electronegativity ( $\chi$ ), ionization potential (I), electron affinity (A) the electrophilicity index ( $\omega$ ), chemical potential ( $\mu$ ),  $\Delta E_{\text{Back-donation}}$ , total energy ( $E_{\text{total}}$ ) and the fraction of electrons transferred ( $\Delta N$ ) from the tetrazole molecule to Copper. The local reactivity has been analysed by means of the Fukui indices, since they indicate the reactive region, in the form of nucleophilic and electrophilic behaviour of each atom in the molecule.

## 2. DFT Calculation

Density functional theory (DFT) methods were employed to study the inhibition efficiency of tetrazole-1 and tetrazole-2. The DFT is one of the quantum chemical methods, used for the evaluation of corrosion inhibitors. It has shown significant promise and appears to be adequate for pointing out the changes in electronic structure responsible for inhibitor action [19]. The energy of the fundamental state of a polyelectronic system by DFT can be expressed as the total electron density, and in fact, use of electron density instead of a wave function for calculating the energy constitutes the fundamental basis of DFT [20]. In the present study calculations were performed using Gaussian 09w program package [16]. Geometry optimizations were conducted by DFT using Becke's three parameter exchange functional (B3) [17], and includes a mixture of HF with DFT exchange terms associated with the gradient correlated correlation functional of Lee, Yang and Parr (LYP) [18] and the 6-311+G(d,p) basis set.

## RESULTS AND DISCUSSION

### 3.1. Theoretical calculation

The quantum chemical calculations have been widely used to study the reaction mechanism and to interpret the experimental result as well as to solve chemical ambiguities [21]. Frontier molecular orbital, HOMO and LUMO were used to predict the adsorption centres of the inhibitor molecule. For the simplest transfer of electron, adsorption should occur at the part of the molecule where the softness,  $\sigma$ , which is a local property, has the highest value. According to Koopman's theorem [22], the energies of the HOMO and LUMO orbitals of the inhibitor molecule are related to the ionization potential, I, and the electron affinity, A, respectively, by the following relationship.

$$I = -E_{\text{HOMO}} \quad (1)$$

$$A = -E_{\text{LUMO}} \quad (2)$$

Absolute electronegativity,  $\chi$ , and absolute hardness,  $\eta$  of the inhibitor molecule are given [23]

$$\chi = I + A/2 \quad (3)$$

$$\eta = I - A/2 \quad (4)$$

The softness is the inverse of the hardness [23]

$$\sigma = 1/\eta \quad (5)$$

Electronegativity, hardness, and softness have proved to be very useful quantities in chemical reactivity theory. When two systems Copper and inhibitor, are brought together, electrons will flow from inhibitor which possesses lower  $\chi$  to the Copper having high  $\chi$ , until the chemical potential becomes equal. The number of transferred electron ( $\Delta N$ ) was also calculated by using the equation below [22].

$$\Delta N = \chi_{\text{Cu}} - \chi_{\text{inh}}/2(\eta_{\text{Cu}} + \eta_{\text{inh}}) \quad (6)$$

Where  $\chi_{\text{Cu}}$  and  $\chi_{\text{inh}}$  denote the absolute electronegativity of copper and inhibitor molecule, respectively,  $\eta_{\text{Cu}}$  and  $\eta_{\text{inh}}$  denote the absolute hardness of copper and the inhibitor molecule respectively. In this study, we use the theoretical value of  $\chi_{\text{Cu}} = 4.98$  eV [24] and  $\eta_{\text{Cu}} = 0$  by assuming that for a metallic bulk  $I = A$  [25] because they are softer than the neutral metallic atoms.

The Fukui function, which measures the sensitivity of a system's chemical potential to an external perturbation at a particular site, is defined as [26, 27].

$$f(r) = (\partial\rho(r) / \partial N)_{v(r)} = (\delta\mu / \delta v(r))_N \quad (7)$$

Since the above derivatives are discontinuous, three different types of Fukui function have been defined [28-30]. They are as follows:

for nucleophilic attack

$$f^+(r) = \rho_{N+1}(r) - \rho_N(r) \quad (8a),$$

for electrophilic attack

$$f^-(r) = \rho_N(r) - \rho_{N-1}(r) \quad (8b)$$

and for radical attack

$$f^0(r) = (\rho_{N+1}(r) - \rho_{N-1}(r))/2 \quad (8c)$$

Parr et al, [31] introduced the global electrophilicity index ( $\omega$ ) in terms of chemical potential and hardness as

$$\omega = \mu^2/2\eta \quad (9)$$

The simple charge transfer model for donation and back-donation of charges proposed recently by Gomez et al., [32] gives the information that the electronic back-donation process might be occurring governing the interaction between the inhibitor molecule and the metal surface. The concept establishes that if both processes occur, namely charge transfer to the molecule and back-donation from the molecule, the energy change is directly related to the hardness of the molecule, as indicated in the following expression.

$$\Delta E_{\text{Back-donation}} = -\eta/4 \quad (10)$$

The  $\Delta E_{\text{Back-donation}}$  implies that when  $\eta > 0$  then  $\Delta E_{\text{Back-donation}} < 0$  and the charge transfer to a molecule, followed by back-donation from the molecule is energetically favoured. In this context, hence, it is possible to compare the stabilization among inhibiting molecules, since there will be an interaction with the same metal, then it is expected that it will decrease as the hardness increases.

### 3.2. Theoretical findings

The chemical structure of tetrazole-1 and tetrazole-2 are shown in **figure-1** and the optimized molecular structure shown in **figure-2**. The inhibition of copper has been investigated theoretically using tetrazole-1 and tetrazole-2 corrosion inhibitors and the results are presented in table-1. The calculated values of  $E_{\text{HOMO}}$ ,  $E_{\text{LUMO}}$ , dipole moment and energy gap of the investigated inhibitor obtained from Gaussian 09w using DFT/B3LYP/6-311G(d,p) are given in **table-1**. According to the frontier molecular orbital theory (FMO) of chemical reactivity, transition of electron is due to the interaction between HOMO and LUMO of reacting species [33]. The energy of the highest occupied molecular orbital ( $E_{\text{HOMO}}$ ) measures the tendency towards the donation of electron by a molecule. Hence, higher values of  $E_{\text{HOMO}}$  indicate better tendency towards the donation of electron, enhancing the adsorption of the inhibitor on Copper and therefore better inhibition efficiency.  $E_{\text{LUMO}}$  indicates the ability of a molecule to accept electrons. The binding ability of the inhibitor to the metal surface increases with increasing of HOMO and decreasing the LUMO energy values.

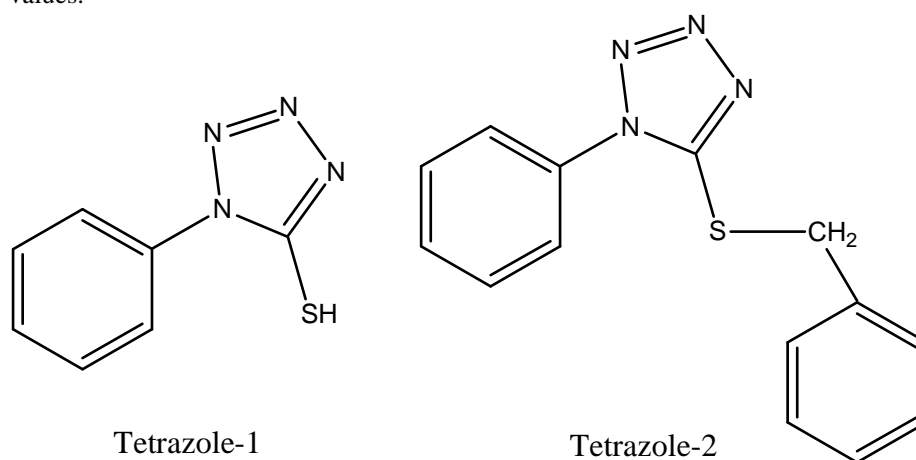


Figure-1: Chemical structure of 1-Phenyl-1,2,3,4-tetrazole-5-thiol (Tetrazole-1) and 5-Benzylthio-1-phenyl-1,2,3,4-tetrazole (Tetrazole-2)

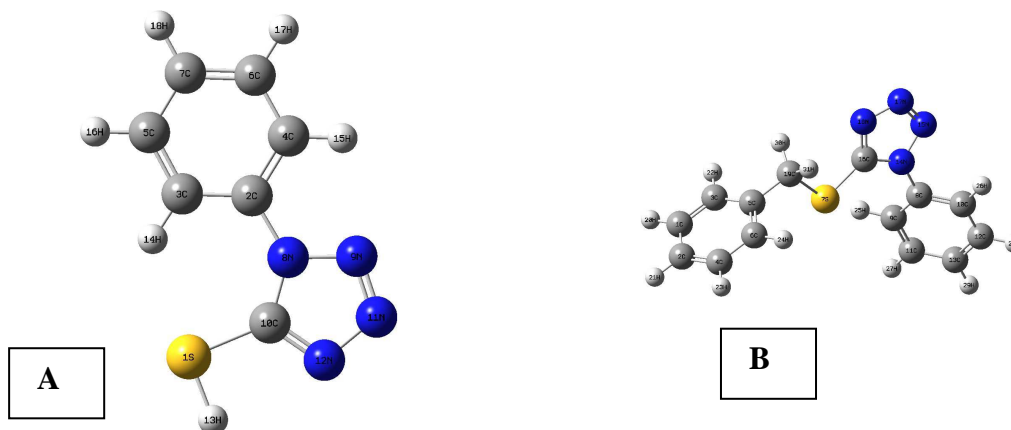


Figure-2: Optimized molecular structure of Tetrazole-1 (A) and Tetrazole-2 (B) obtained at B3LYP/6-311G(d,p) level

The molecule with the highest  $E_{\text{HOMO}}$  value often has the highest tendency to donate electrons to appropriate acceptor molecule of low empty molecular orbital energy [34]. The inhibitor not only donate electron to the unoccupied d orbital of the metal ion but can also accept electron from the d-orbital of the metal leading to the formation of a feed back bond. The highest value of  $E_{\text{HOMO}}$  -6.4922 eV of tetrazole-1 indicates its better inhibition efficiency than the other inhibitor tetrazole-2.

### 3.3. Frontier molecular orbital (FMO)

The energy gap between the HOMO and LUMO, ( $\Delta E$ ) provide information about the overall reactivity of the molecule. The higher value of  $\Delta E$  leads to decrease in the inhibition efficiency of the molecule [35]. The lower the values of the ( $\Delta E = E_{\text{HOMO}} - E_{\text{LUMO}}$ ) energy gap the better will be the inhibition efficiency since the energy required to remove an electron from the last occupied orbital will be minimum [36]. In the present investigation  $\Delta E$  values obtained was follows the order Tetrazole-1 < Tetrazole-2, suggesting that the inhibitor Tetrazole-1 has the highest reactivity and would therefore likely to interact strongly with the metal surface.

### 3.4. Ionization energy

The ionization energy is a fundamental descriptor of the chemical reactivity of atoms and molecules. High ionization energy indicates high stability and chemical inertness and small ionization energy indicates high reactivity of the atom and molecules [37]. The low value of ionization energy 6.4922 (eV) of tetrazole-1 indicates that the tetrazole-1 possesses high inhibition efficiency.

### 3.5. Dipole moment

The dipole moment ( $\mu$  in Debye) is another important electronic parameter which provides the information on the polarity and the reactivity indicator of the molecule. Literature survey reveals that several irregularities appeared in case of correlation of dipole moment with inhibitor efficiency [38]. The values obtained for tetrazole-1 and tetrazole-2 does not reflect any significant relationship between the dipole moment values and inhibition efficiencies [39].

### 3.6. Electronegativity

The electronegativity ( $\chi$ ) values displayed in table-1 shows that tetrazole-2 has higher electronegativity value compared to tetrazole-1. Hence, the difference in the electronegativity values between the metal and the inhibitor is in the following order tetrazole-1 > tetrazole-2. According to Sanderson's electronegativity equalization principle [40], tetrazole-2 with a high electronegativity value and lower difference in electronegativity value between the metal and the tetrazole-2 definitely reaches equalization quickly and hence low reactivity is expected which in turn indicates low inhibition efficiency of tetrazole-2.

### 3.7. Hardness and softness

Absolute hardness ( $\eta$ ) and softness ( $\sigma$ ) are important properties to measure the molecular stability and reactivity. The obvious property is chemical hardness fundamentally signifies the resistance towards the deformation or

polarization of the electron cloud of the atoms, ions or molecules under small perturbation of chemical reaction. A hard molecule has a large energy gap and a soft molecule has a small energy gap [41]. The calculated results of tetrazole-1 with low hardness value  $\eta = 2.54485$  eV compared to that of the tetrazole-2  $\eta = 2.5880$  eV has a low energy gap. In general, the inhibitor with the least value of absolute hardness (that is highest value of absolute softness) is expected to have the highest inhibition efficiency [42]. Tetrazole-1 with the high softness value of 0.39295 eV has the highest inhibition efficiency compared to tetrazole-2 which has lower value of 0.3864 eV (**table-1**).

### 3.8. Number of electrons transferred

The number of electrons transferred ( $\Delta N$ ) was calculated and the results are tabulated in **table-2**. If  $\Delta N$  is less than 3.6, the inhibition efficiency increases due to the increase in the electron-donating ability of the inhibitor to the metal surface [43] and it increases in the following order tetrazole-1 > tetrazole-2. The highest fraction of electron transfer can be correlated to the inhibitor efficiency while the lowest fraction of electron transfers lower inhibition efficiency. In the present study the tetrazole-1 with the highest fraction of electron transfer ( $\Delta N = 0.202890$  eV) will exhibit higher inhibition efficiency than the tetrazole-2, which has lower fraction of electron transfer ( $\Delta N = 0.12562$  eV).

### 3.9. Electrophilic index ( $\omega$ )

The electrophilic index,  $\omega$ , shows the ability of the inhibitor molecules to accept electrons. It is a measure of the stabilization in energy after a system accepts additional amount of electron charge from the environment [44]. The electron donating ( $\omega^-$ ) and electron accepting ( $\omega^+$ ) powers have been defined as [45].

$$\omega^- = (3I + A)^2 / 16(I-A) \quad (11)$$

and

$$\omega^+ = (I + 3A)^2 / 16(I-A) \quad (12)$$

It follows that a larger  $\omega^+$  value corresponds to a better capability of accepting charge, whereas a smaller value of  $\omega^-$  value of the system makes it a better electron donor. The results obtained shows that tetrazole-1 is found to be the strongest nucleophile than tetrazole-2. In order to compare  $\omega^+$  with  $\omega^-$ , the following definition of net electrophilicity has been proposed [46].

$$\Delta\omega^\ddagger = \omega^+ - (-\omega^-) = \omega^+ + \omega^-$$

that is electron accepting power relative to the electron donating power. The electron donating ( $\omega^-$ ) and electron accepting ( $\omega^+$ ) powers and net electrophilicity  $\Delta\omega^\ddagger$  of tetrazole-1 and tetrazole-2 are presented in **table-3**.

**Table-1: Quantum chemical parameters for Tetrazole-1 and Tetrazole-2 calculated using B3LYP/6-311G(d,p)**

Parameters	Tetrazole-1	Tetrazole-2
Enthalpy of formation	-887.6313 au	-1157.9341 au
Dipole moment (Debye)	4.8086	5.1813
HOMO (eV)	-6.4922	-6.9178
LUMO (eV)	-1.40250	-1.7418
Ionization Potential (I) eV	6.4922	6.9178
Electron affinity (A) eV	1.40250	1.7418
Energy gap ( $\Delta E$ )	5.0897	5.1760
Hardness ( $\eta$ ) eV	2.54485	2.5880
Global Softness ( $\sigma$ ) eV	0.39295	0.3864
Electrophilic index ( $\omega$ ) eV	3.06139	3.6219
Electronegativity ( $\chi$ ) eV	3.94735	4.3298
Chemical Potential ( $\mu$ ) eV	-3.94735	-4.3298

**Table-2: The number of electron transferred ( $\Delta N$ ) and  $\Delta E_{\text{Back donation}}$  (eV) calculated for inhibitor Tetrazole-1 and Tetrazole-2**

Parameters	Tetrazole-1	Tetrazole-2
Transferred electron fraction ( $\Delta N$ ) (eV)	0.202890	0.12562
$\Delta E_{\text{Back donation}}$ (eV)	-0.6362125	-0.6470

In **table-2**, the calculated  $\Delta E_{\text{Back-donation}}$  values for the inhibitors are presented. The magnitude of the values shows that  $\Delta E_{\text{Back-donation}}$  for tetrazole-1 higher than tetrazole-2, which indicates that back-donation, is favoured for the

tetrazole-1, a characteristic feature of a best inhibitor. The  $\Delta E_{\text{Back-donation}}$  implies that when  $\eta > 0$  and  $\Delta E_{\text{Back-donation}} < 0$  then the charge transfer to a molecule, followed by a back donation from the molecule is energetically favoured [47].

### 3.10. Local reactivity

The condensed Fukui functions allow us to distinguish each part of the molecule on the basis of its distinct chemical behaviour due to the different substituent functional groups. The condensed dual descriptor has been defined as  $f^{(2)}(r)_k = f_k^+ - f_k^-$  [48]. From the interpretation given to the Fukui function, one can note that the sign of the dual descriptor is very important to characterize the reactivity of a site within a molecule toward a nucleophilic or an electrophilic attack. That is, if  $f^{(2)}(r)_k > 0$ , then the site is favoured for a nucleophilic attack, whereas if  $f^{(2)}(r)_k < 0$ , then the site may be favoured for an electrophilic attack [49,50].

The calculated values of  $f^+$  and  $f^-$  for tetrazole-1 and tetrazole-2 are presented in **table-4** and **table-5** respectively. In this study a large negative value of the condensed dual descriptor  $f^{(2)}(r)$  over S1, implies that this will be preferred site for the electrophilic attack. The density functional predicts that C10 will be preferred site of nucleophilic attack for tetrazole-1. Similarly, S1 will be the preferred site of electrophilic attack and C16 will be the preferred site of nucleophilic attack.

**Table-3: Electron donating ( $\omega^-$ ) and electron accepting ( $\omega^+$ ) powers and net electrophilicity ( $\Delta\omega^\pm$ ) of Tetrazole-1 and Tetrazole-2 calculated with the B3LYP density functional and the 6-311G(d,p) basis set**

Property	Tetrazole-1	Tetrazole-2
$\omega^-$ (eV)	4.01145	4.3644
$\omega^+$ (eV)	1.40582	1.78054
$\Delta\omega^\pm$ (eV)	5.417274	6.14494

**Figure-3: Frontier molecular orbitals (FMO) of Tetrazole-1 and Tetrazole-2 molecules calculated at B3LYP/6-311+G(d,p) level of theory**

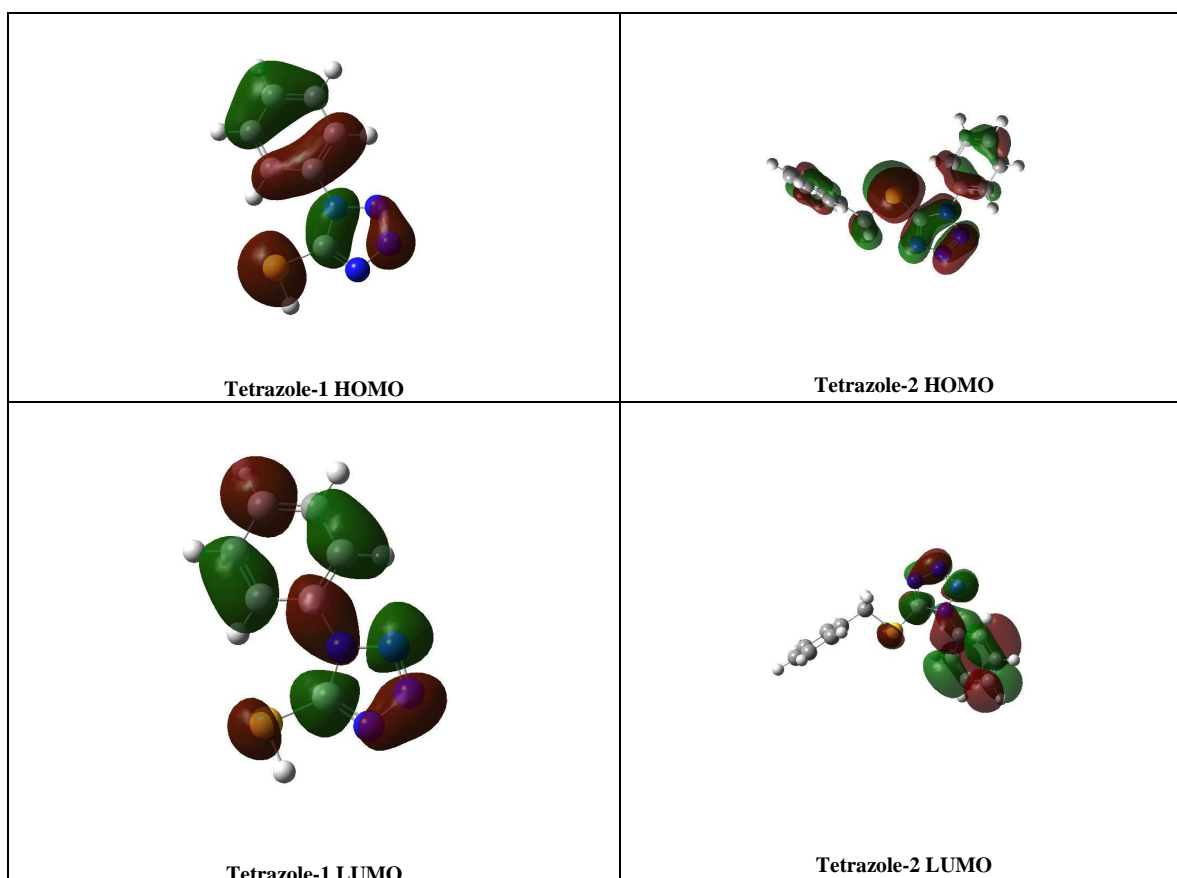


Table-4: Electrophilic  $f^+$  and nucleophilic  $f^-$  condensed fukui functions and  $f^{(2)}(r)$  over the atoms of the Tetrazole-1 molecule calculated with Calculation B3LYP density functional and 6-311G (d,p) basis set

Atoms		$f^+$	$f^-$	$f^{(2)}(r)$	$f^o$
1	S	0.18548	0.24871	-0.0632	0.217098
2	C	0.14033	-0.0486	0.18893	0.045862
3	C	0.06102	-0.0038	0.06489	0.028573
4	C	0.12266	0.01874	0.10392	0.070696
5	C	0.04498	0.00898	0.036	0.026982
6	C	0.02857	0.01327	0.0153	0.020921
7	C	0.18861	0.01181	0.17681	0.100211
8	N	-0.0693	-0.0367	-0.0325	-0.05304
9	N	0.10948	-0.0270	0.13653	0.041215
10	C	0.21829	-0.0339	0.25219	0.092192
11	N	0.11858	0.07462	0.04396	0.096601
12	N	0.03732	0.02804	0.00929	0.03268
13	H	0.05405	0.05635	-0.0023	0.055199
14	H	0.06563	0.04469	0.02093	0.055161
15	H	0.0623	0.05729	0.00501	0.059792
16	H	0.09435	0.07532	0.01903	0.08483
17	H	0.09439	0.07584	0.01855	0.085112
18	H	0.10471	0.08347	0.02124	0.094094

Table-5: Electrophilic  $f^+$  and nucleophilic  $f^-$  condensed fukui functions and  $f^{(2)}(r)$  over the atoms of the Tetrazole-2 molecule calculated with Calculation B3LYP density functional and 6-311G (d,p) basis set

Atoms		$f^+$	$f^-$	$f^{(2)}(r)$	$f^o$
1	C	0.0078	0.01889	-0.01109	0.026696
2	C	0.09403	0.01825	0.07578	0.112287
3	C	0.07484	-0.0031	0.07793	0.07174
4	C	0.07423	0.01967	0.05456	0.093901
5	C	0.03183	-0.08326	0.11509	-0.05142
6	C	-0.00172	-0.00719	0.00547	-0.00891
7	S	0.14753	0.24851	-0.10098	0.396041
8	C	0.07388	-0.08137	0.15525	-0.00748
9	C	0.00953	-0.02487	0.0344	-0.01535
10	C	0.0994	0.01222	0.08719	0.111621
11	C	0.06077	0.0178	0.04297	0.078574
12	C	0.01678	0.0229	-0.00611	0.03968
13	C	0.15628	0.01818	0.1381	0.174451
14	N	-0.03477	-0.01409	-0.02067	-0.04886
15	N	0.08331	0.01501	0.0683	0.098317
16	C	0.09905	-0.06687	0.16592	0.032181
17	N	0.07997	0.05394	0.02603	0.133912
18	N	0.02029	0.01503	0.00526	0.035315
19	C	0.01988	-0.04445	0.06433	-0.02457
20	H	0.05355	0.0528	0.00075	0.10635
21	H	0.05853	0.05229	0.00624	0.110824
22	H	0.03796	0.03645	0.0015	0.074409
23	H	0.05404	0.05159	0.00244	0.10563
24	H	0.03606	0.0357	0.00036	0.071753
25	H	0.04401	0.01726	0.02675	0.061274
26	H	0.05734	0.03607	0.02127	0.093405
27	H	0.06918	0.04701	0.02217	0.116191
28	H	0.07351	0.05186	0.02165	0.125365
29	H	0.07941	0.0555	0.02391	0.134905
30	H	0.05781	0.06953	-0.01172	0.127338
31	H	0.04528	0.07521	-0.02993	0.120484

Figure-4: ESP maps for the optimized Tetrazole-1 and Tetrazole-2 neutral N (A), N-1 (B) and N+1(C)

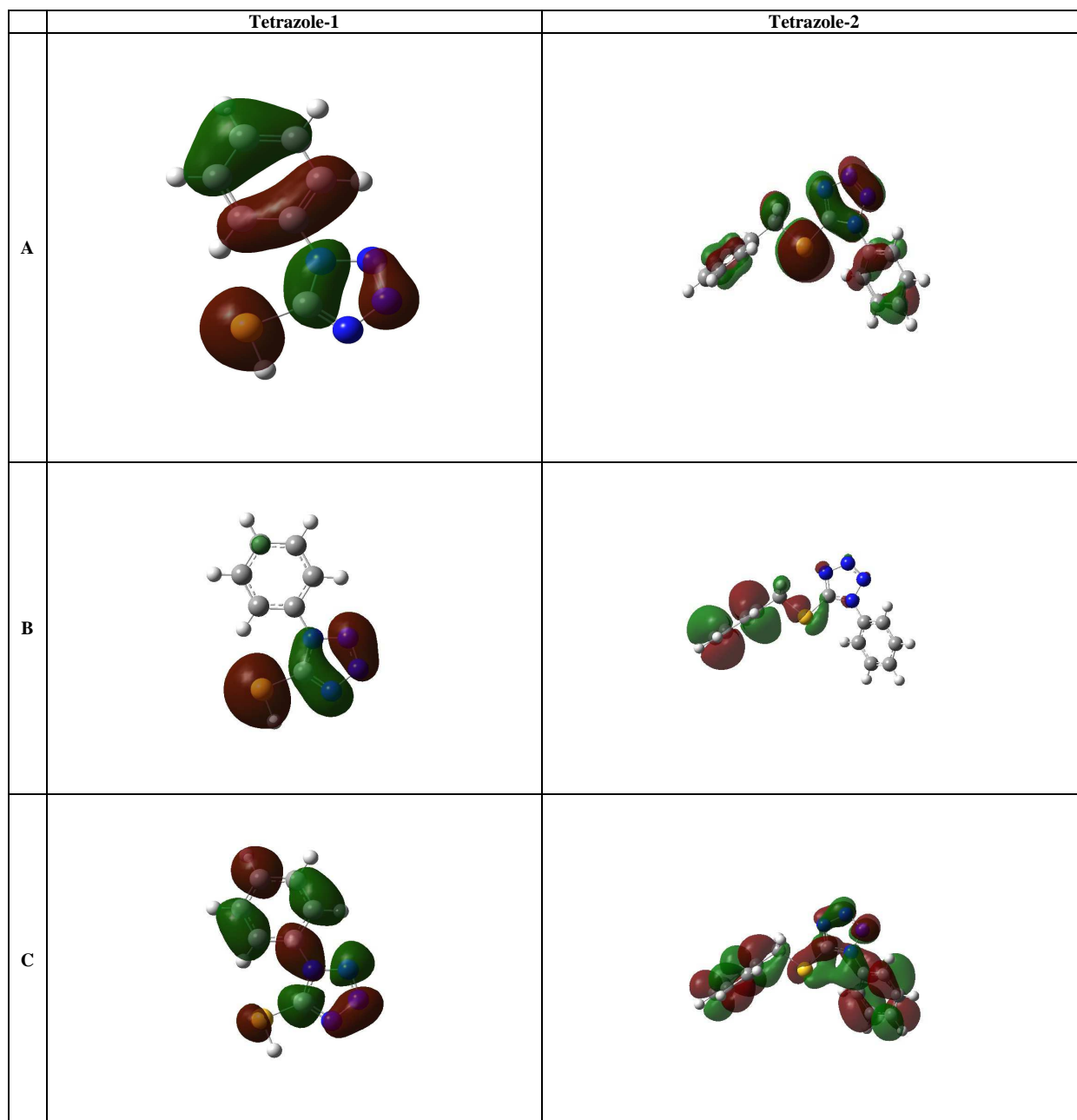
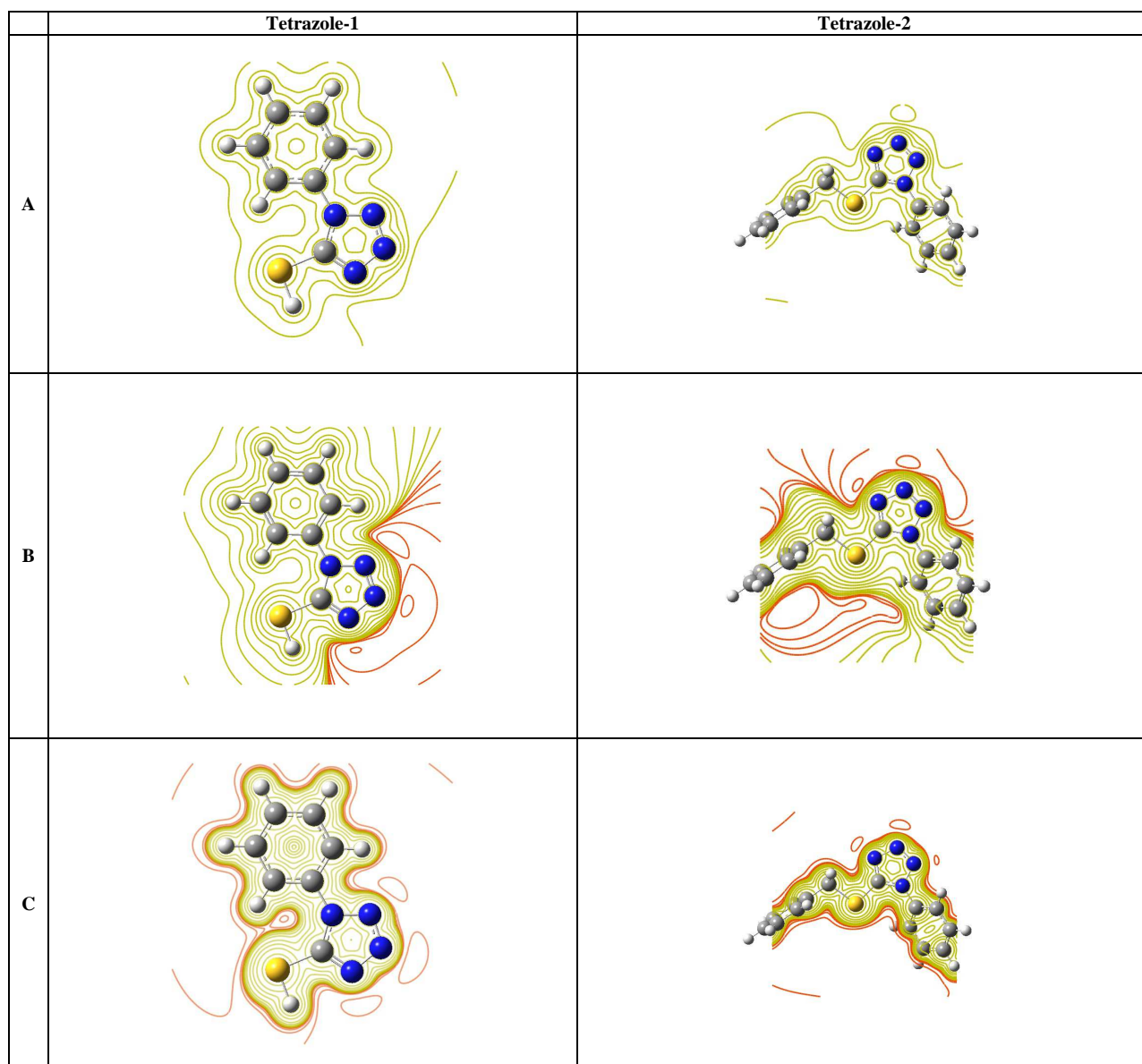


Figure-5: Isosurface map for the highest occupied molecular orbital (HOMO) density squared with contour value of 0.02 of the optimized conformer of neutral (A) and positively charged (B) and negatively charged (C) Tetrazole-1 and Tetrazole-2



The HOMO and LUMO orbitals of tetrazole-1 and tetrazole-2 are presented in **figure-3**. The information obtained from the HOMO and LUMO orbitals are consistent with the findings obtained from the Fukui function. The nucleophilic Fukui function and electrophilic Fukui function of tetrazole-1 and tetrazole-2 are correlated with ESP (**figure-4**) and contour maps (**figure-5**).

### CONCLUSION

Quantum chemical calculations, using the DFT, have been performed on tetrazole derivatives, tetrazole-1 and tetrazole-2 to investigate their geometric and electronic properties in an attempt to elucidate the reactivity and selectivity centres of the compounds. The inhibition efficiency of tetrazole-1 was found to be higher than tetrazole-2. Fukui function shows the nucleophilic and electrophilic attacking sites of the inhibitor tetrazole-1 and tetrazole-2.

### REFERENCES

- [1] EA Noor; *J. Eng. Appl. Sci.*, **2008**, 3, 23-30
- [2] EE Ebenso; NO Eddy; AO Odongenyi, *Afri. J. Pure Appl. Chem.*, **2008**, 4, 107-115
- [3] EE Oguzie, *Pigment Resin Technol.*, **2006**, 35, 334-340
- [4] AS Abdul-Nabi; EQ Jasim, *Int. J. Eng. Research*, **2014**, 3, 613-620

- [5] JL Mora-Mendoza; JG Chacon-Nava; G. Navala-Obivares; MA Gonzalez-Nunez & S. Turgoose, *Corros. Eng.*, **2002**, 58, 608-619
- [6] Y Ahmed; AAH Kadhum; AB Mohamad; MS Takriff, *Corros. Sci.*, **2010**, 52, 3331-3340
- [7] EM Sherif; RM Erasmus; JD Comins, *J. Colloid Interface Sci.*, **2007**, 311, 144-151
- [8] KF Khaled; SA Fadl-Allah; B Hammouti, *Mater. Chem. Phys.*, **2009**, 117, 148-155
- [9] Gy Vastag; E Szocs; A Shaban; E Kalman, *Pure Appl. Chem.*, **2001**, 73, 1861-1869
- [10] M Itoch; H Nishihara; K Aramaki, *J. Electrochem. Soc.*, **1994**, 141, 2018-2033
- [11] Y Yamamoto; H Nishihara; K Aramaki, *J. Electrochem. Soc.*, **1993**, 140, 432-436
- [12] I Lukovitis; I Bako; A Shaban; E Kalman, *Electrochem. Acta*, **1998**, 43, 131-136
- [13] T Arslan; F Kandemirli; EE Ebenso; II Love; H Alemu, *Corrosion Sci*, **2008**, 51, 35
- [14] SL Li; YG Wang; SH Chen; R Yu; SB Lei; HY Ma; DX Liu, *Corrosion Sci.*, **1999**, 41, 1769-1782
- [15] L Vera; MGYP Ortega-Luoni, *Chilean Chem. Soc.*, **2006**, 51, 1034-1035
- [16] Gaussian 09, M. J. Frisch, G. W. Trucks, H. B. Schlegel, G. E. Scuseria, M. A. Robb, J. R. Cheeseman, G. Scalmani, V. Barone, B. Mennucci, G. A. Petersson, H. Nakatsuji, M. Caricato, X. Li, H. P. Hratchian, A. F. Izmaylov, J. Bloino, G. Zheng, J. L. Sonnenberg, M. Hada, M. Ehara, K. Toyota, R. Fukuda, J. Hasegawa, M. Ishida, T. Nakajima, Y. Honda, O. Kitao, H. Nakai, T. Vreven, J. A. Montgomery, Jr., J. E. Peralta, F. Ogliaro, M. Bearpark, J. J. Heyd, E. Brothers, K. N. Kudin, V. N. Staroverov, R. Kobayashi, J. Normand, K. Raghavachari, A. Rendell, J. C. Burant, S. S. Iyengar, J. Tomasi, M. Cossi, N. Rega, J. M. Millam, M. Klene, J. E. Knox, J. B. Cross, V. Bakken, C. Adamo, J. Jaramillo, R. Gomperts, R. E. Stratmann, O. Yazyev, A. J. Austin, R. Cammi, C. Pomelli, J. W. Ochterski, R. L. Martin, K. Morokuma, V. G. Zakrzewski, G. A. Voth, P. Salvador, J. J. Dannenberg, S. Dapprich, A. D. Daniels, Ö. Farkas, J. B. Foresman, J. V. Ortiz, J. Cioslowski and A. D. J. Fox, Gaussian, Inc., Wallingford, **2009**, p. 09
- [17] AD Becke, *Physical Review A*, **1998**, 38, 3098-3100
- [18] C Lee; W Yang; RG Parr, *Physical Review B*, **1988**, 37, 785-789
- [19] P Udhayakala; TV Rajendiran; S Gunasekaran, *J. Adv. Sci. Res.*, **2012**, 67, 1655-1814
- [20] A Zarrouk; I Warad; B Hammouti; A Dafalil; SS Al-Deyab; N Benchat, *Int. J. Electrochem. Sci.*, **2010**, 5, 1516-1526
- [21] A Zarrouk; H Zarrok; R Salghi; B Hammouti; SS Al-Deyab; R Touzani; M Bouachrine; I Wrad; TB Hadda, *Int. J. Electrochem. Sci.*, **2012**, 7, 6353-6364
- [22] RG Pearson, "Absolute Electronegativity and Hardness: Application to Inorganic Chemistry," *Inorganic Chemistry*, 1988, 27, 734-740
- [23] RG Parr; RG Pearson, *J. Am. Chem. Soc.*, **1983**, 105, 7512-7516
- [24] EG Demissie; SB Kassa; G W Woyessa, *Int. J. Sci and Eng. Res.*, **2014**, 5, 304-310
- [25] MJS Dewar; W Thiel, *J. Am. Chem. Soc.*, **1977**, 99, 4899-4907
- [26] RG Parr; W Yang, *J. Am. Chem. Soc.*, **1984**, 106, 4049-4050
- [27] K Fukui, *Science*, **1987**, 218, 747-754
- [28] W Yang; WJ Mortier, *J. Am. Chem. Soc.*, **1986**, 108, 5708-5711
- [29] C Lee; W Yang; RG Parr, *J. Mol. Struct. (Theochem)*, **1988**, 163, 305-313
- [30] J Cioslowski; M Martinov; ST Mixon, *J. Phys. Chem.*, **1993**, 97, 10948-10951
- [31] RG. Parr; LV Szentpaly; S Liu, *J. Am. Chem. Soc.*, **1999**, 121, 1922-1924
- [32] B Gomez; NV Likhanova; MA Dominguez-Aguilar; R Martinez-palou; AVela, J Gazquez, *J. Phy. Chem. B*, **2006**, 110, 8928-8934.
- [33] P Udhayakal TV Rajendiran; SJ Gunasekaran, *Adv. Sci. Res.*, **2012**, 3, 67-74
- [34] G Gece; S Bilgic, *Corros. Sci.*, **2009**, 51, 1876-1878
- [35] MK Awad; MR Mustafa; MM Abo Elnga, *J. Mol. Struct. (Theochem)*, **2010**, 959, 66-74
- [36] CO Akalezi; CK Enenebaku; EE Oguize, *Int. J. of Indus. Chem.*, **2012**, 3, 13-25
- [37] T Chakraborty; DC Ghosh, *Mol. Phy.*, **2010**, 108, 2018-2092
- [38] G Gece, *Corros. Sci.*, **2008**, 50, 2981-2992.
- [39] X Li; S Deng; H Fu; T. Li, *Electrochim. Acta*, **2009**, 54, 4089-4098
- [40] P Geerlings; FD Profit, *Int. J. Mol. Sci.*, **2002**, 3, 276-309
- [41] NO Obi-Egbedi; IB Obot; MI El-Khaiary; SA Umoren; EE Ebenso, *Int. J. Electrochem. Sci.*, **2011**, 6, 5649-5675
- [42] EE Ebenso; DA Isabirye; NO Eddy, *Int. J. Mol. Sci.*, 2010, 11, 2473-2498
- [43] I Lukovits; E Kalman; F Zucchi, *Corrosion*, **2001**, 57, 3-8
- [44] S Liu, *J. Chem. Sci.*, **2005**, 117, 477-483
- [45] JL Gazquez; A Cedillo; A Vela, *J. Phys. Chem. A*, **2007**, 111, 1966-1970.
- [46] PK Chattaraj; A Chakraborty; S Giri, *J. Phy. Chem. A.*, **2009**, 113, 10068-10074
- [47] P Udhayakala; TV Rajendiran; S Gunasekaran, *J. Chem. Bio. Phy. Sci. Sec. A*, **2012**, 2, 1151-1165
- [48] C Morell; A Grand; A Toro-Labbe, *Chem. Phys. Lett.*, **2006**, 425, 342-346
- [49] J Gazquez, *J. Phys. Chem. A*, **1997**, 101, 4657-4659

[50] JL Gazquez, Chemical reactivity concepts in density functional theory. In chemical reactivity theory: A density functional view. Edited by P.K. Chattaraj, Boca Raton: CRC Press-Taylor & Francis Group, 2009, 7-21.